Supporting information

Dynamic dual-atom synergetic catalysis boosted by liquid metal for direct seawater electroreduction

Haoxuan Li [a], *Jinghui Wang* [a,*], *Mei Cui* [b], *Renliang Huang* [a, c,*], *Wei Qi* [b], *Rongxin Su* [a, b, c,*]

[a] Tianjin Key Laboratory for Marine Environmental Research and Service, School of Marine Science and Technology, Tianjin University, Tianjin 300072, P.R. China

[b] State Key Laboratory of Chemical Engineering, Tianjin Key Laboratory of Membrane Science and Desalination Technology, School of Chemical Engineering and Technology, Tianjin University, Tianjin 300072, P.R. China

[c] Zhejiang Institute of Tianjin University, Ningbo, Zhejiang 315201, P.R. China

* Author to whom correspondence should be addressed:

wjh1031@tju.edu.cn (J.Wang), tjuhrl@tju.edu.cn (R. Huang), surx@tju.edu.cn (R. Su)

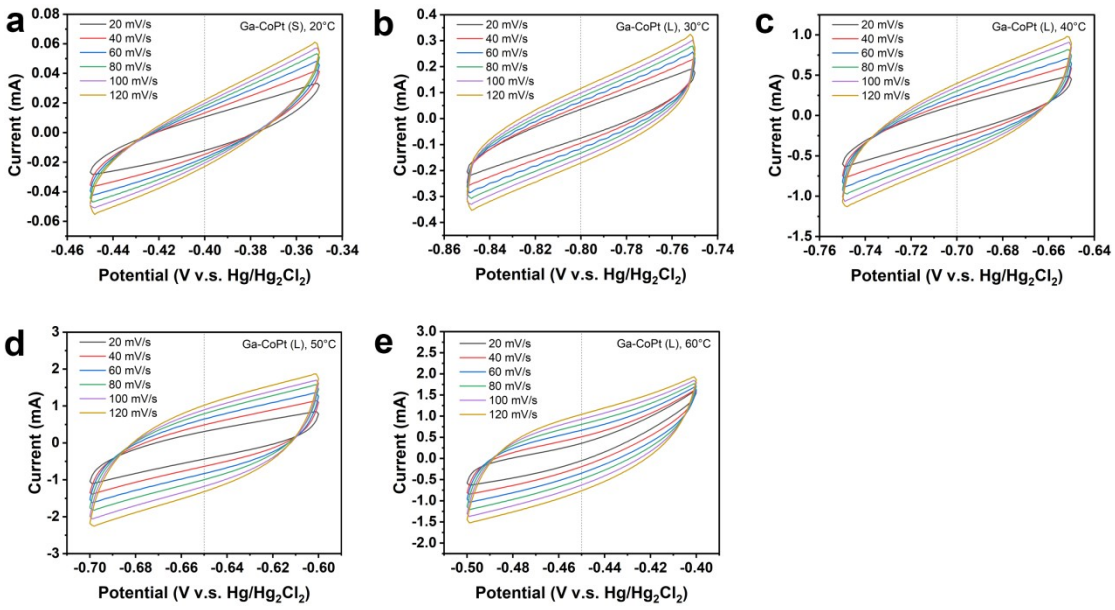

Fig. S1. Electrochemical active surface area of Ga-CoPt determined by cyclic voltammetry (CV) measurements at a scan rate of 20, 40, 60, 80, 100 and 120 mV/s in the non-faradaic potential range. (**a** to **e**) CV curves of Ga-CoPt at (**a**) 20 °C (Solid), (**b**) 30 °C (Liquid), (**c**) 40 °C (Liquid), (**d**) 50 °C (Liquid) and (**e**) 60 °C (Liquid).

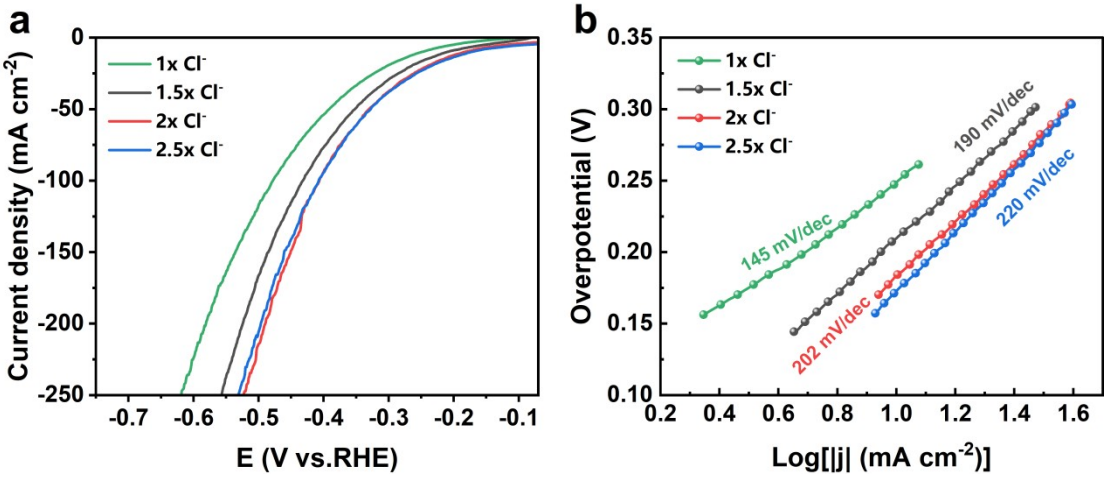

Fig. S2. (**a**) LSV curves of Ga-CoPt at 50 °C in natural seawater and 1.5 times, 2 times, 2.5 times of Cl^- concentration. (**b**) The corresponding Tafel plots derived from the LSV curves.

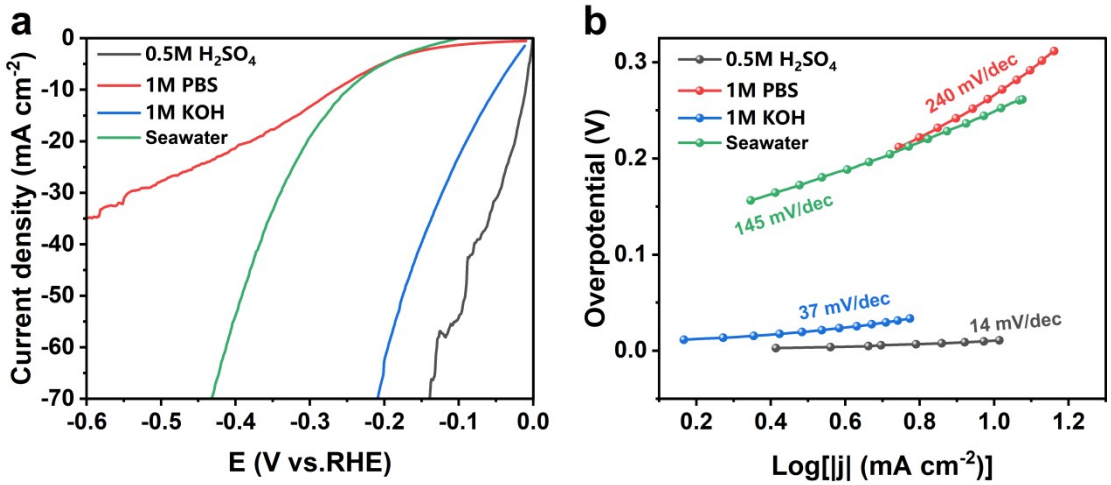

Fig. S3. (**a**) LSV curves of liquid Ga-CoPt in natural seawater, 0.5 M H_2SO_4, 1 M PBS and 1 M KOH electrolytes at 50 °C. (**b**) The corresponding Tafel plots derived from the LSV curves.

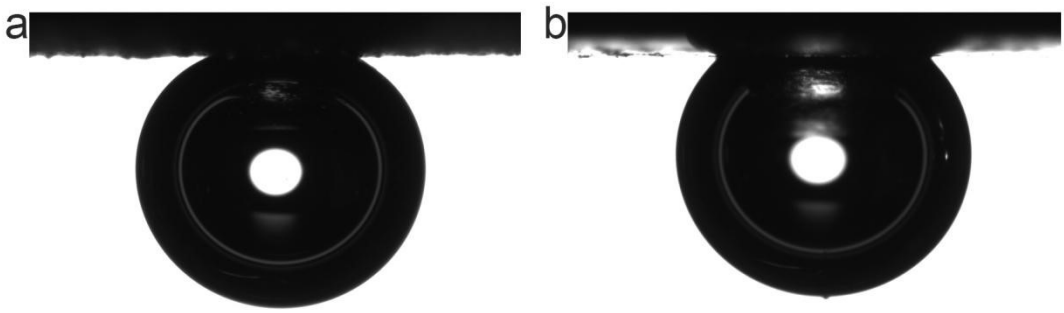

Fig. S4. Bubble contact angles of (**a**) liquid Ga-CoPt (164.3 ± 2.3°) and (**b**) Pt/C (140.0 ± 2.2°) under seawater.

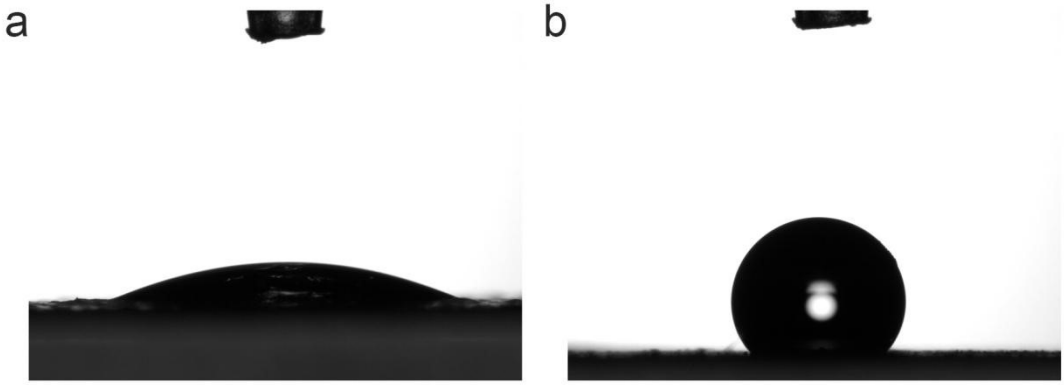

Fig. S5. Seawater contact angles of (**a**) liquid Ga-CoPt (23.6 ± 1.8°) and (**b**) Pt/C (129.7 ± 1.9°).

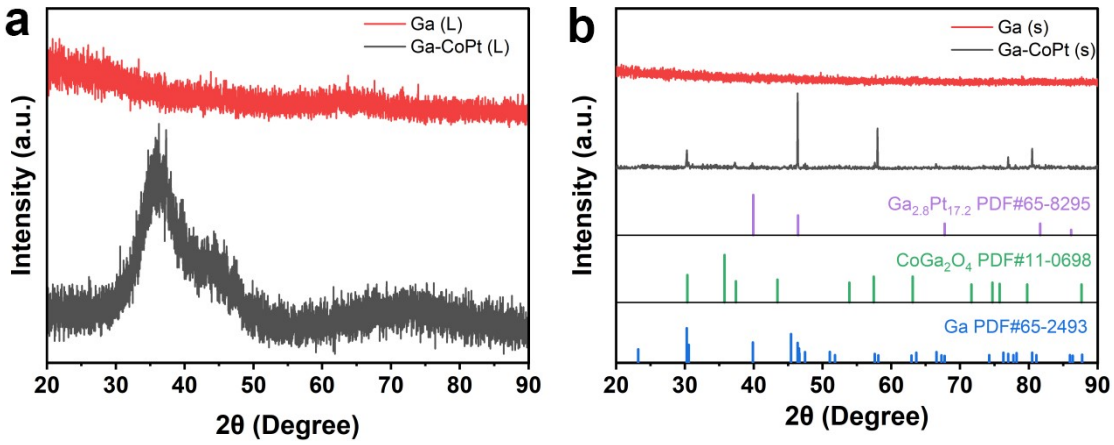

Fig. S6. XRD patterns of (**a**) liquid Ga and Ga-CoPt and (**b**) solid Ga and Ga-CoPt.

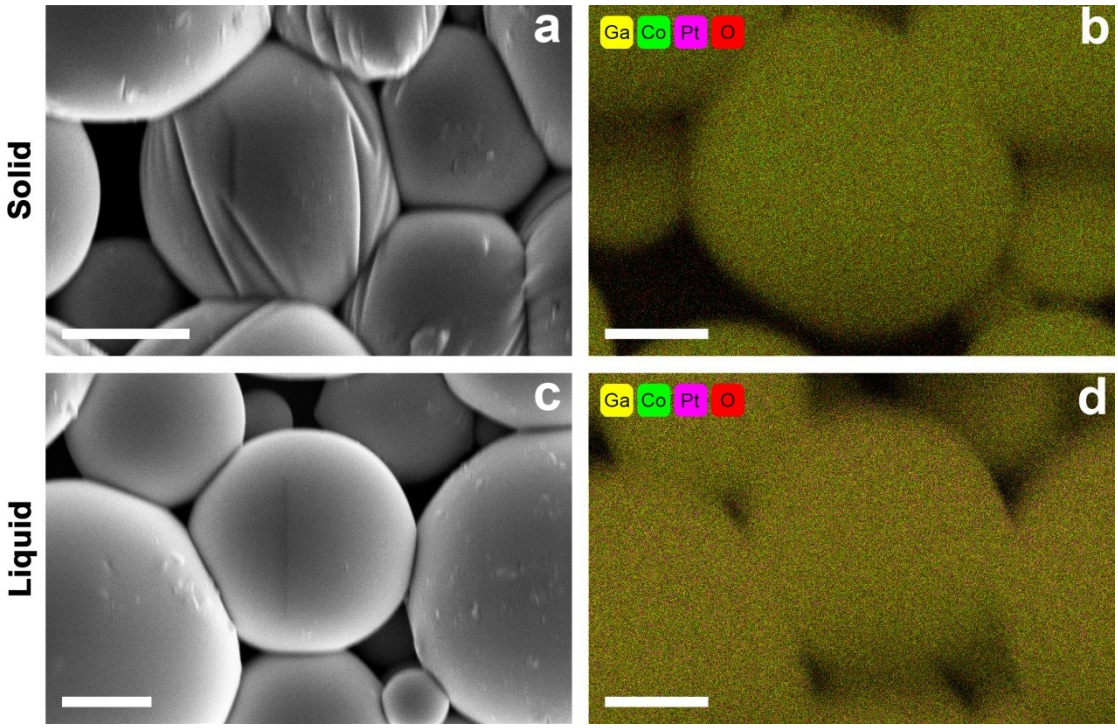

Fig. S7. SEM images and EDS mapping of solid and liquid Ga-CoPt. SEM images of (**a**) solid and (**c**) liquid Ga–CoPt. EDS mapping of (**b**) solid and (**d**) liquid Ga-CoPt. The scale bar in (**a-d**) is 1 μm.

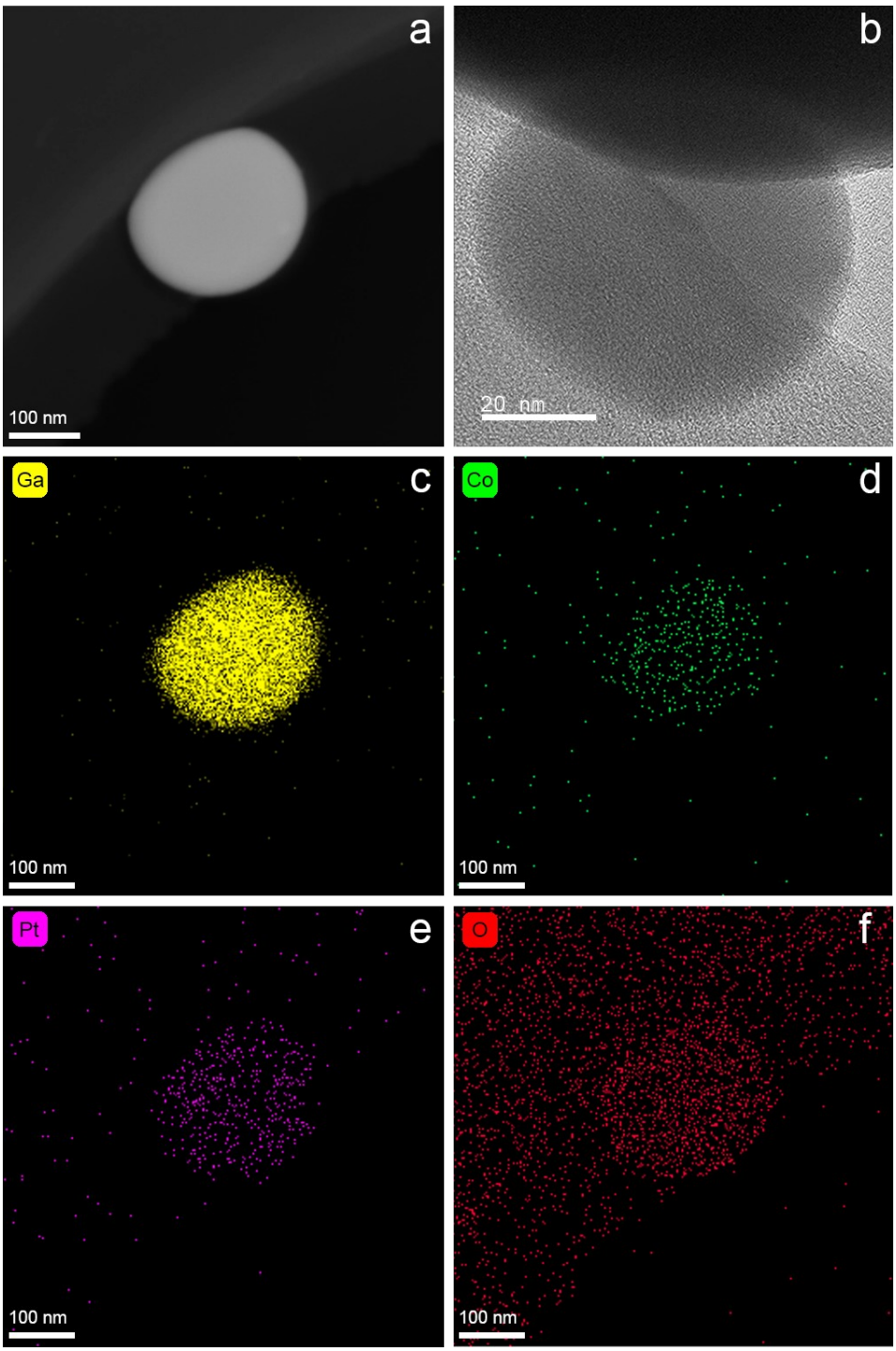

Fig. S8. Characterizations of the liquid Ga-CoPt after the stability test. (**a**) HAADF image of liquid Ga-CoPt. (**b**) HRTEM image of liquid Ga-CoPt. (**c** to **f**) STEM images for the spatial distribution of Ga, Co, Pt, O elements in liquid Ga-CoPt.

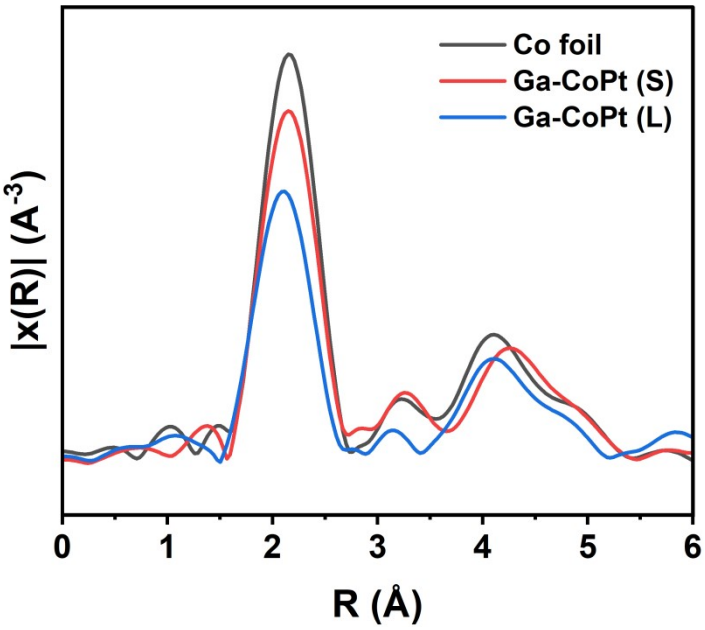

Fig. S9. R-space of Co K-edge EXAFS spectra of solid and liquid Ga-CoPt.

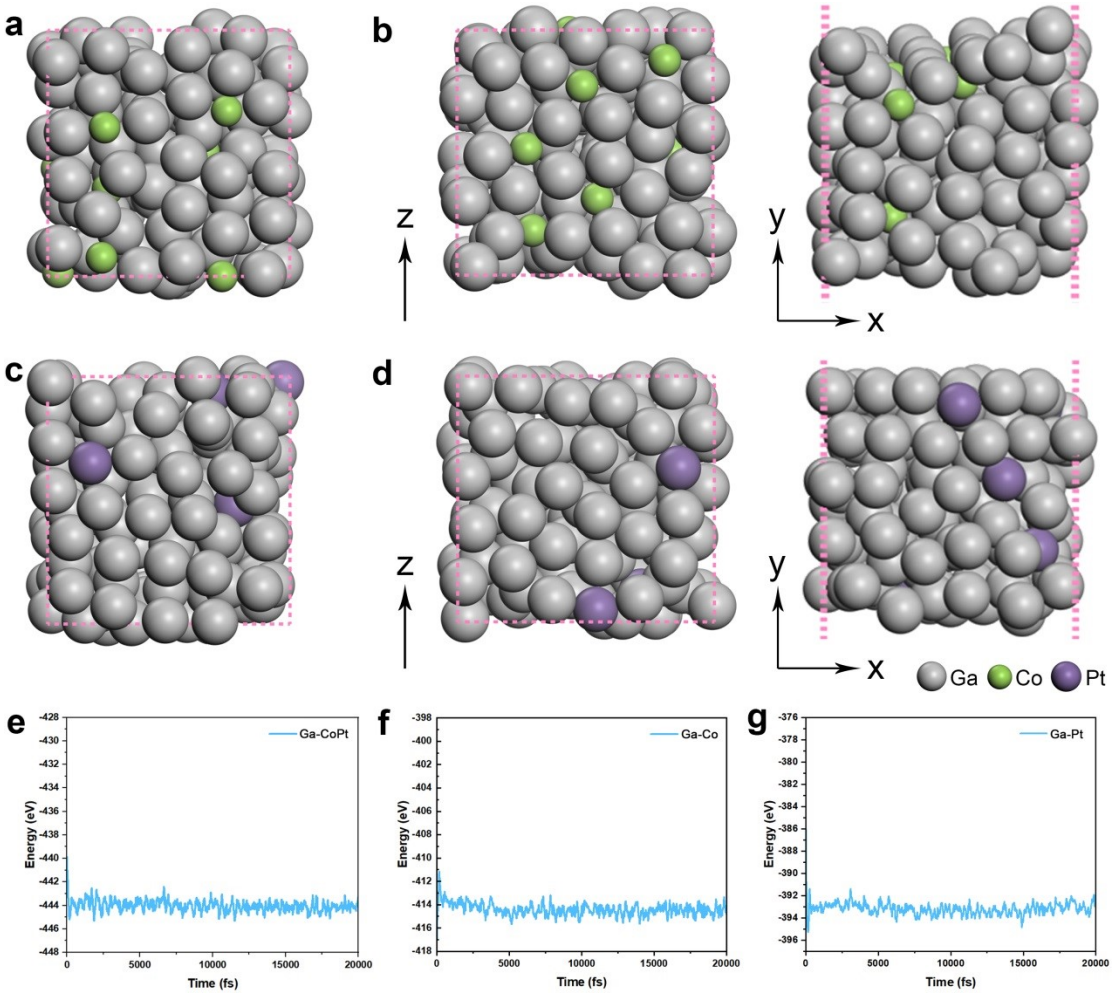

Fig. S10. Ab initio molecular dynamic simulation of Ga-CoPt, Ga-Co and Ga-Pt at 323.15 K. Representative snapshots of atomic configurations at (**a**) bulk of Ga-Co, (**b**) interface of Ga-Co, (**c**) bulk of Ga-Pt and (**d**) interface of Ga-Pt. Stability of (**e**) Ga-CoPt, (**f**) Ga-Co, (**g**) Ga-Pt models at 323.15K.

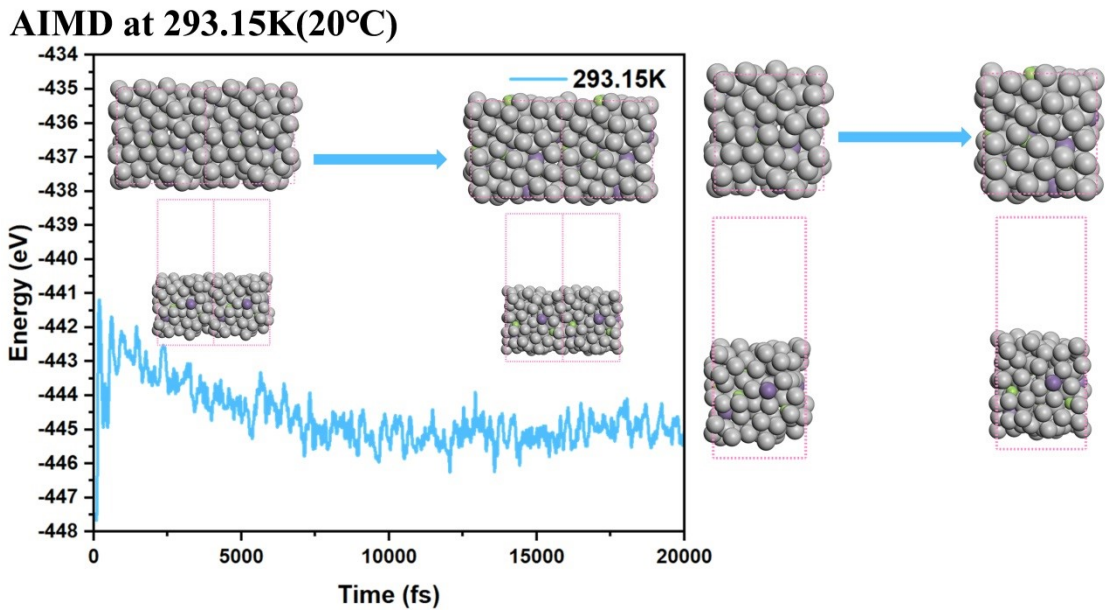

Fig. S11. Ab initio molecular dynamics simulation of Co and Pt atoms in solid Ga at 293.15 K. After 20000 fs the system is stabilized and the Co and Pt atoms are still encapsulated in Ga.

Table S1. The comparison of electrocatalytic performance with previous reported work for direct seawater reduction.

Catalyst	η_{10} (mV)	η_{10} of 20% Pt/C (mV)	Tafel slope (mV dec^{-1})	Durability (h)	Maximum stabilized current density (mA cm^{-2})	Ref.
Ga-CoPt at 50 °C	249	341	145	169	-100	This work
Ga-CoPt at 60 °C	208		175			
$Ni_{2.4}Co_{1.6}N$/NC	256	~230	94.1	2	-200	[1]
Ti@$Ni(OH)_2$-NiMoS	371	~370	162	12	-10	[2]
$La_{0.17}Mo_{0.83}P$/PC/MXene	158	263	-	400	-100	[3]
P-doped NiSe	296	-	180	100	-100	[4]
Ni/V_2O_3-4	221	-	-	-	-	[5]
C–MoCSx@MoS_2	312	~300	128	-	-	[6]
NiMo@C_3N_5	486	264	-	10	-10	[7]
Co-FePO/OH	~250	~180	-	10	-10	[8]
NF@Mo-$Ni_{0.85}Se$	~370	~330	183.7	12	-10	[9]
N-Co-S/G	~450	~280	341.2	15	-20	[10]
CoNiP/Co_xP	290	-	-	500	-10	[11]
Fe-Co_2P	489	275	-	100/48	-40/-200	[12]

NiCoN|NixP|NiCoN	165	90	139.2	24	10	[13]
Pt_{at}-CoP MNSs	~300	~330	-	24	Potential=-0.5 (V vs RHE)	[14]
2.4% Pt@mh-3D MXene	280	308	-	250	-10	[15]
VS_2@V_2C	η_{20}=444	η_{20}=428	160	200	-150	[16]
NiRuIr-G	~200	-	-	-	-	[17]
Mn–Ni–S/NF-3	301	~220	-	20	-15	[18]
$Co_{0.31}Mo_{1.69}C$/MXene/NC	312	~300	-	225	-40	[19]
NP-MoS_2/CC	345.4	~290	-	8	-10	[20]
NiCoP/NF	287	~290	-	-	-	[21]
0.5Rh-GS1000	320	303	-	10	-10	[22]
NPNNS	144	121	108	10	-100	[23]
MoS_2QD-aerogel-100	~350	~200	-	-	-	[24]

Table S2. The mass of the electrodes before and after the HER stability tests.

	Mass of electrode (g)
Before	0.1245
After	0.1174
Leakage ratio	5.7 %

References

1 D. Zhang, Y. Zhou, D. Liu, C. Song and D. Wang, *J. Colloid. Interf. Sci.*, 2023, **629**, 873-881.

2 C. Yang, L. Zhou, T. Yan, Y. Bian, Y. Hu, C. Wang, Y. Zhang, Y. Shi, D. Wang, Y. Zhen and F. Fu, *J. Colloid. Interf. Sci.*, 2022, **606**, 1004-1013.

3 X. Wu, J. Qiu and Z. Wang, *Small Struct*, 2022, **4**, 2200268.

4 M. Maleki, A. Sabour Rouhaghdam, G. Barati Darband, D. Han, M. Chehelamirani and S. Shanmugam, *J. Electroanal. Chem.*, 2022, **916**, 116379.

5 G. Liu, H. Lv, Q. Quan, X. Li, H. Lu, W. Li, X. Cui and L. Jiang, *Chem. Eng. J.*, 2022, **450**, 138079.

6 Y. Li, S. Zuo, Q. Li, H. Huang, X. Wu, J. Zhang, H. Zhang and J. Zhang, *Appl. Catal. B: Environ.*, 2022, **318**, 121832.

7 X. Bu, X. Liang, Y. Bu, Q. Quan, Y. Meng, Z. Lai, W. Wang, C. Liu, J. Lu, C.-M. Lawrence Wu and J. C. Ho, *Chem. Eng. J.*, 2022, **438**, 135379.

8 Q. Zhang, Z. L. Zhe Ru, R. Daiyan, P. Kumar, J. Pan, X. Lu and R. Amal, *ACS Appl. Mater. Inter.*, 2021, **13**, 53798-53809.

9 C. Yang, C. Wang, L. Zhou, W. Duan, Y. Song, F. Zhang, Y. Zhen, J. Zhang, W. Bao, Y. Lu, D. Wang and F. Fu, *Chem. Eng. J.*, 2021, **422**, 130125.

10 P. Sabhapathy, I. Shown, A. Sabbah, P. Raghunath, J.-L. Chen, W.-F. Chen, M.-C. Lin, K.-H. Chen and L.-C. Chen, *Nano Energy*, 2021, **80**, 105544.

11 D. Liu, H. Ai, M. Chen, P. Zhou, B. Li, D. Liu, X. Du, K. H. Lo, K. W. Ng, S. P. Wang, S. Chen, G. Xing, J. Hu and H. Pan, *Small*, 2021, **17**, 2007557.

12 Y. Lin, K. Sun, X. Chen, C. Chen, Y. Pan, X. Li and J. Zhang, *J. Energy Chem.*, 2021, **55**, 92-101.

13 L. Yu, L. Wu, S. Song, B. McElhenny, F. Zhang, S. Chen and Z. Ren, *ACS Energy Lett.*, 2020, **5**, 2681-2689.

14 S. Ye, W. Xiong, P. Liao, L. Zheng, X. Ren, C. He, Q. Zhang and J. Liu, *J. Mater. Chem. A*, 2020, **8**, 11246-11254.

15 L. Xiu, W. Pei, S. Zhou, Z. Wang, P. Yang, J. Zhao and J. Qiu, *Adv. Funct. Mater.*, 2020, **30**, 1910028.

16 Z. Wang, W. Xu, K. Yu, Y. Feng and Z. Zhu, *Nanoscale*, 2020, **12**, 6176-6187.

17 M. Sarno, E. Ponticorvo and D. Scarpa, *Electrochem. Commun.*, 2020, **111**, 106647.

18 L. Zeng, Z. Liu, K. Sun, Y. Chen, J. Zhao, Y. Chen, Y. Pan, Y. Lu, Y. Liu and C. Liu, *J. Mater. Chem. A*, 2019, **7**, 25628-25640.

19 X. Wu, S. Zhou, Z. Wang, J. Liu, W. Pei, P. Yang, J. Zhao and J. Qiu, *Adv. Energy Mater.*, 2019, **9**, 1901333.

20 K. Sun, L. Zeng, S. Liu, L. Zhao, H. Zhu, J. Zhao, Z. Liu, D. Cao, Y. Hou, Y. Liu, Y. Pan and C. Liu, *Nano Energy*, 2019, **58**, 862-869.

21 Q. Lv, J. Han, X. Tan, W. Wang, L. Cao and B. Dong, *ACS Appl. Energy Mater.*, 2019, **2**, 3910-3917.

22 Y. Liu, X. Hu, B. Huang and Z. Xie, *ACS Sustain. Chem. Eng.*, 2019, **7**, 18835-18843.

23 Y. Huang, L. Hu, R. Liu, Y. Hu, T. Xiong, W. Qiu, M. S. Balogun, A. Pan and Y. Tong, *Appl. Catal. B: Environ.*, 2019, **251**, 181-194.

24 I. P. Chen, C. H. Hsiao, J. Y. Huang, Y. H. Peng and C. Y. Chang, *ACS Appl. Mater. Inter.*, 2019, **11**, 14159-14165.